

# Dynamic Coloration of Complex Emulsions by Localization of Gold Rings Near the Triphase Junction

Kang Hee Ku, Benjamin R. McDonald, Harikrishnan Vijayamohanam,  
Cassandra A. Zentner, Sara Nagelberg, Mathias Kolle, and Timothy M. Swager\*

Multiphase microscale emulsions are a material platform that can be tuned and dynamically configured by a variety of chemical and physical phenomena, rendering them inexpensive and broadly programmable optical transducers. Interface engineering underpins many of these sensing schemes but typically focuses on manipulating a single interface, while engineering of the multiphase junctions of complex emulsions remains underexplored. Herein, multiphilic triblock copolymer surfactants are synthesized and assembled at the triphase junction of a dynamically reconfigurable biphasic emulsion. Tailoring the linear structure and composition of the polymer surfactants provides affinity to each phase of the complex emulsion (hydrocarbon, fluorocarbon, and continuous water phase), yielding selective localization of polymers around the triphase junction. Conjugation of these polymers with gold nanoparticles, forming structured rings, affords a dynamic reflected isotropic structural color that tracks with emulsion morphology, demonstrating the uniquely enabling nature of a functionalized triphase interface. This color is the result of interference of light along the internal hydrocarbon/fluorocarbon interface, with the gold nanoparticles scattering and redirecting light into total internal reflection competent paths. Thus, the functionalization of the triphase junction renders complex emulsions colorimetric sensors, a powerful tool toward sensitive and simple sensing platforms.

## 1. Introduction

Fluid interfaces offer a convenient and versatile template for the construction of structures and functional materials.<sup>[1]</sup> The macroscopic, planar interface between two immiscible liquids (e.g., water and oil) has been widely exploited in the bottom-up preparation of functional membranes and ordered thin films through interfacial polymerization<sup>[1c,2]</sup> and assembly of amphiphilic polymers<sup>[3]</sup> or nanoparticles (NPs)<sup>[4]</sup> extending to macroscopic geometric areas. The fabrication of nanostructures consisting of functional NPs is of particular interest to create systems with desirable optical, electrical, and catalytic properties.<sup>[5]</sup> In contrast to the planar interfaces of macroscopic liquid–liquid mixtures, dispersed complex microscale emulsions provide a substantially greater interfacial area, as well as dynamic and reconfigurable active surfaces with a rich variety of nonplanar configurations and interfacial kinetics.<sup>[6]</sup> Furthermore, the interfaces of multiphase emulsions possess unique optical properties dependent on interface configuration and particle orientation.<sup>[7]</sup> Responsive surfactants create


interfaces that can be programmed to selectively reconfigure to a specific physical or chemical entity, rendering multiphase emulsions versatile chemo-optical transducers for a variety of sensing platforms.<sup>[8]</sup> As such, the ability to manipulate interface morphology and thus properties, hinges upon the ability to selectively functionalize liquid–liquid interfaces.

Although engineering the reactivity of interfaces via surfactant design has been broadly explored, attention has been primarily focused on a single external interface, i.e., where one phase interacts with the continuous phase. Recently, attention has turned to the design of polymer surfactants that accumulate at internal interfaces in multiphase emulsions, enabling precise modulation of interfacial tension between inner phases of complex emulsions (i.e., the interface between two different oils in an aqueous continuous phase).<sup>[9]</sup> However, many opportunities afforded by the assembly of molecules along the interface of all phases in biphasic aqueous emulsions, the “*triphase junction*,” have yet to be explored. Specifically, the ability to manipulate

Prof. K. H. Ku, Dr. B. R. McDonald, Dr. H. Vijayamohanam,  
C. A. Zentner, Prof. T. M. Swager  
Department of Chemistry  
Massachusetts Institute of Technology (MIT)  
77 Massachusetts Ave., Cambridge, MA 02139, USA  
E-mail: tswager@mit.edu

Prof. K. H. Ku  
Department of Chemical Engineering and Applied Chemistry  
Chungnam National University  
Daejeon 34134, Republic of Korea

Dr. S. Nagelberg, Prof. M. Kolle  
Department of Mechanical Engineering  
Massachusetts Institute of Technology (MIT)  
77 Massachusetts Ave., Cambridge, MA 02139, USA

 The ORCID identification number(s) for the author(s) of this article can be found under <https://doi.org/10.1002/smll.202007507>.

DOI: 10.1002/smll.202007507

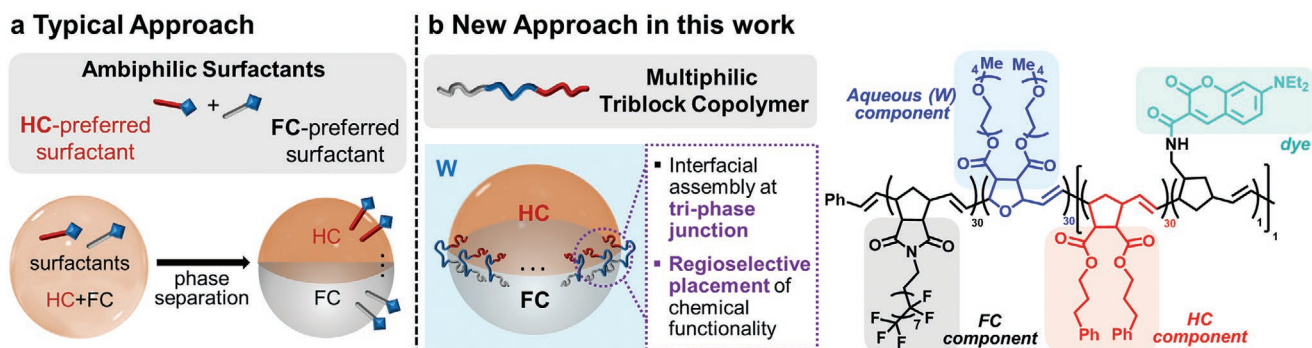


**Figure 1.** a) Use of amphiphilic surfactants to control the shape of biphasic emulsions composed of hydrocarbon (HC) and fluorocarbon (FC). b) Schematic illustration for the reconfiguration of double emulsion from core/shell (HC/FC/W or FC/HC/W) to Janus shape driven by a localized assembly of triBCPs at the triphase junction, and chemical structure of the triBCP surfactants containing FC, HC, and aqueous components.

and instill functionality at multiphase liquid interfaces would facilitate exciting opportunities to modulate interface morphology, instill new transduction mechanisms, and ultimately realize new functional materials. Surfactant design is the key to realize new functions in such systems. Polymeric surfactants are widely used to stabilize functional emulsion interfaces and can be broadly varied in chemical functionality. They are highly mobile at the fluid interfaces, and achieve an equilibrium assembly.<sup>[10]</sup> To date, the design of polymeric surfactants for emulsions has primarily focused on aqueous amphiphilic systems, where the molecular assembly occurs at the oil/water interfaces.<sup>[10a]</sup> Given the facile and broad tailorability of polymers, multiphilic polymeric surfactants should be accessible by simple molecular design.

In this study, we localize multiphilic ABC linear triblock copolymers (triBCPs) at the triphase junction of biphasic emulsions to manipulate the emulsions' morphology and optical characteristics. Our approach offers a simple and modular synthetic route for tailoring the interfacial balance between three immiscible liquids to enable localization of chemical and optical functionality. The triBCP is composed of three different blocks that each has a selective affinity to either the fluorocarbon (FC), hydrocarbon (HC), or water (W) phase (**Figure 1**). Rapid interface localization of triBCPs results in their selective assembly along the triphase junction to minimize overall interfacial energies, and can thereby transform an emulsion that would otherwise prefer a core/shell structure into a Janus configuration. As described herein, we demonstrate that the linear configuration and concentration of triBCPs can be used to control the shape of the emulsions. Additionally, the unique functionality engendered by selective functionalization of the triphase interface is demonstrated with gold nanoparticles (Au NPs), serving as a template for the formation of a gold ring at the emulsions' triphase junction. The size and thickness of this gold ring can be dynamically tuned by the external chemical environment. We show that strong light scattering by the gold rings funnels light into total internal reflection (TIR) competent paths with associated optical interference and isotropizes the structural colors that can be generated at the internal, concave optical interface of emulsions. The dynamic nature of the emulsion-gold ring system allows visualization and quantitative determination of changes in emulsion shape through the reflected color. This

striking phenomenon is rationalized analytically by considering the light scattering characteristics of the Au NPs and its effect on the color generation by TIR and interference, allowing us to theoretically explain the modulation of the reflected color as a function of the shape of the biphasic emulsion.

## 2. Results and Discussion

### 2.1. Self-Assembly of Triblock Copolymers at the Junction of Three Immiscible Liquids

Our strategy to selectively localize polymer surfactants at the junction of three immiscible liquids is founded on the design of ABC triBCPs containing HC, FC, and aqueous (W) components. To ensure homogenous, molecule-like surfactant performance, a robust living polymerization is required.<sup>[11]</sup> Taking into account the broad functional group tolerance, simplicity of functional monomer synthesis, and ability to rapidly generate block structures, ruthenium-catalyzed ring-opening metathesis polymerization (ROMP) was chosen to prepare the desired triBCPs.<sup>[12]</sup> Given that an ABC block copolymer can have three different linear structures (ignoring chain-end functionality), we were unsure of how this structural variation would affect polymer assembly at the triphase junction and the resulting consequence on emulsion morphology. Thus, a series of three different polymers having the same building blocks, relative compositions, and molecular weights, but different linear structures were prepared. For convenience, we denote each triBCP using the center block (e.g., W block-centered triBCP as W-triBCP), as depicted in **Figure 2**.

To ensure facile polymer and emulsion preparation, a modest molecular weight of approximately 50 kDa was targeted. Finally, to track polymer localization, a strong blue-emitting coumarin dye comonomer was incorporated into the HC block of each polymer. Each polymer was obtained in modest to good yield and narrow dispersity (70%, number-average molecular weights ( $M_n$ ) = 45.5 kDa,  $\mathcal{D}$  = 1.14 for HC-triBCP; 42%,  $M_n$  = 47.4 kDa,  $\mathcal{D}$  = 1.10 for FC-triBCP; 76%,  $M_n$  = 38.9,  $\mathcal{D}$  = 1.14 for W-triBCP) (See Supporting Information for further details).

A series of biphasic emulsions containing different concentrations of W-triBCP, HC-triBCP, and FC-triBCP surfactants

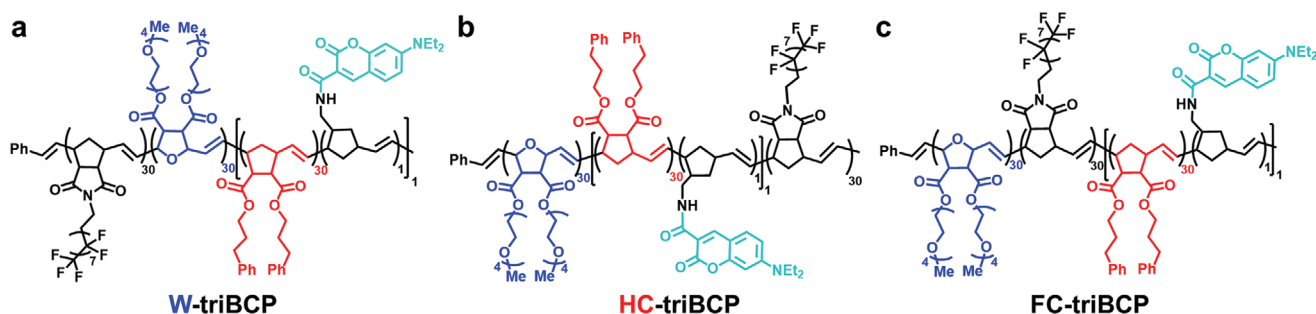


**Figure 2.** Chemical structures of triBCPs having different linear configurations of a) W block-centered triBCP (W-triBCP), b) HC block-centered triBCP (HC-triBCP), and c) FC block-centered triBCP (FC-triBCP).

from 0 to 0.3 wt% were prepared. A dichloromethane (DCM) solution of triBCP was mixed with HC (i.e., diethylbenzene) and FC (i.e., HFE-7500) above their upper critical solution temperature of 40 °C, and was then emulsified in a 0.5 wt% aqueous solution of Zonyl FS-300 (Zonyl is a non-ionic fluorosurfactant with a linear chemical formula of  $F(CF_2)_xCH_2CH_2O(CH_2CH_2O)_yH$ ) using microfluidics. Upon cooling and evaporation of the DCM, temperature-induced phase separation yields biphasic emulsions with different Janus configurations depending on the polymer structure and concentration (Figure 3 and Figures S1–S3, Supporting Information). Figure 3a summarizes the effect of the linear structure and concentration of triBCPs on the shape of biphasic emulsions. To quantify the shape of emulsions, we used side-view optical microscopy images to measure the contact angle,  $\theta_{HC}$ , between the HC/W interface and HC/FC interface of the emulsions. Without the triBCP surfactant, a perfect double emulsion with HC core and FC shell was obtained with the Zonyl surfactant stabilizing the FC/W interface. Decreasing values of  $\theta_{HC}$  were observed with an increase in the concentration of polymer regardless of polymer structures, however, a more substantial decrease was observed for FC-triBCPs. For example, for the volume fraction ( $f$ ) of triBCPs at 0.15 wt%, the values of  $\theta_{HC}$  for W-triBCP, HC-triBCP, and FC-triBCP were 117°, 104°, and 77°, respectively. This difference can be rationalized by the molecular configuration of polymers at the emulsion interface as illustrated in Figure 3b. As a result of the high solubility of the

HC component in the oil phase, it is possible that the triBCPs organize to form core/shell micellar structures around the FC-block, resulting in a screening effect via a tightly coiled or intra-block aggregation of the FC-component. In contrast, in the case of W-triBCP, the aqueous building block locates at the center of linear polymer, therefore it is intuitive that the polymer chain will adopt a horseshoe-like shape, possibly rendering the screening effect of FC-component less favorable. By inference, the degree of the screening effect is maximized when the FC-component is at the center of triBCP.

Given that the morphological changes seen with the triBCP polymers are driven by changes in the interfacial tension ( $\gamma$ ) between immiscible liquids,<sup>[10a-c]</sup> and/or line tension at the triphase interface, the surfactant ability of the triBCPs was further quantified by pendant-drop measurements (Table 1). It is important to note that for the HC and FC solvents chosen, the HC/FC interfacial energy is much lower than the corresponding HC/W and FC/W cases (i.e., less than 1 mN m<sup>-1</sup>), and hence will have no role in determining the overall morphology of the biphasic emulsion. HC- and FC-triBCP show strong reductions of  $\gamma$  values at the HC/W interface; However, FC-triBCP provides only a slight reduction (i.e., less than 1 mN m<sup>-1</sup>) of  $\gamma$  at the FC/W interface, which reveals that it behaves as a strong HC-selective surfactant (i.e., the FC block is screened). The reductions of  $\gamma$  at both HC/W and FC/W interface with W-triBCP strongly support the hypothesis that it exhibits a balanced adsorption behavior. For example, at  $f_{W-triBCP} = 0.15$  wt%,

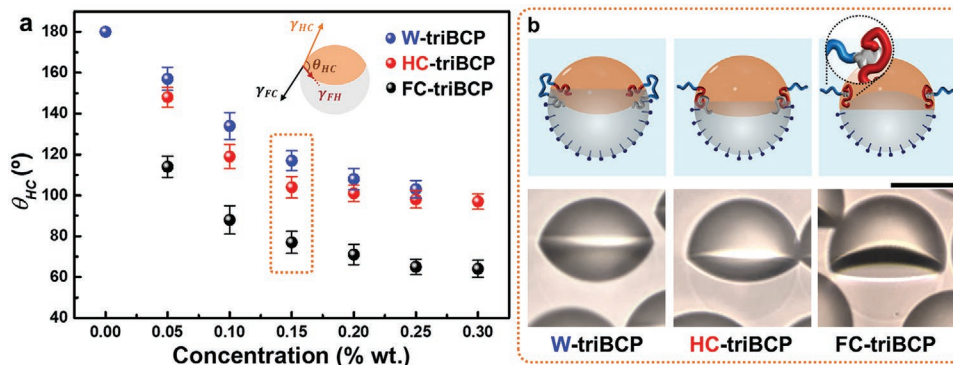


**Figure 3.** Effect of the linear configuration of triBCP on the shape of diethylbenzene/HFE-7500 biphasic emulsions stabilized by Zonyl (0.5 wt%). a) A plot of the angle between HC/W interface and HC/FC interface ( $\theta_{HC}$ ) as a function of the concentration of triBCPs. b) Side-view optical microscopy images of emulsions prepared with 0.15 wt% of each triBCP and corresponding schematic illustration for the molecular configurations of W-, H-, and FC-triBCP at the emulsion interface. Scale bar is 50  $\mu$ m.

**Table 1.** Interfacial tension values ( $\gamma$ ;  $\text{mN m}^{-1}$ ) at HC/W and FC/W interfaces in the presence of triBCP.

Interface	Without polymer	W-triBCP			HC-triBCP (0.15 wt%)	FC-triBCP (0.15 wt%)
		Polymer concentration [wt%]				
		0.05	0.15	0.3		
HC/W	31.28 ( $\pm 1.50$ )	9.74 ( $\pm 0.06$ )	9.29 ( $\pm 0.21$ )	8.33 ( $\pm 0.09$ )	3.51 ( $\pm 0.16$ )	4.59 ( $\pm 0.07$ )
FC/W	49.84 ( $\pm 0.16$ )	35.66 ( $\pm 2.63$ )	28.36 ( $\pm 0.61$ )	21.40 ( $\pm 0.24$ )	34.24 ( $\pm 4.89$ )	49.18 ( $\pm 0.29$ )

a dramatic reduction of surface tension from 31.28 to 9.29  $\text{mN m}^{-1}$  and 49.84 to 28.36  $\text{mN m}^{-1}$  are observed for HC/W and FC/W interfaces, respectively. Moreover, a horseshoe conformation would likely be preferred at the triphase interface. Additionally, W-triBCP is singular in accommodating surfactant-triggered changes in emulsion morphology, whereas emulsions with HC-triBCP or FC-triBCP do not show this property (Figure S4, Supporting Information). This difference may explain the unique ability of the W-triBCP to yield dynamic emulsion configuration.

To visualize the spatial localization of this polymer within the biphasic emulsion, the fluorescence emission of the attached coumarin was utilized in a fluorescent confocal microscope (Figure 4). Top-down images show the W-triBCP localizing only at the interface and not the bulk of the droplet. The aggregated bands have a concentration maximum at the triphase interface and subsequently extend into the HC/W interface reaching up to 20  $\mu\text{m}$  in depth for a 65  $\mu\text{m}$  diameter droplet, potentially acting as a reservoir of materials to the adjacent interface. The triblock nature of the polymer surfactant is key for the dominant segregation to the triphase region. For example, when an analogous diblock polymer surfactant, consisting of only the HC and water-stabilizing blocks, is used with the same loading fraction, the polymer randomly aggregates along the HC/W interface and does not show any preference for localization

around the triphase junction (Figure S5, Supporting Information). Thus, it can be expected that conjugating functional groups to the W-triBCP can be expected to largely localize these groups around the triphase interface.

## 2.2. Fabrication of Gold Ring and Enhancement of Structural Color

With the ability to create a dense band of W-triBCPs around the triphase junction in a biphasic emulsion, we sought to realize new functionality in complex emulsions. Optical metamaterials are composed of uniform arrays of conductive, optically active structures, with rings being an example of such a structure.<sup>[13]</sup> The prospect of creating dynamically reconfigurable conductive rings spurred our interest in using the W-triBCP functionalized biphasic emulsions as a template for such a material system. We thus added a reactive chemical moiety to the W-triBCP in order to bind and localize Au NPs around the triphase junction. Specifically, pentafluorophenol ester comonomers were incorporated into the aqueous block of the W-triBCP (yielding PFP-W-triBCP), which allows grafting of amine-containing materials by amidation reactions.<sup>[14]</sup> Notably, significant amounts (15 units) of this reactive ester could be incorporated without adversely affecting the surfactant

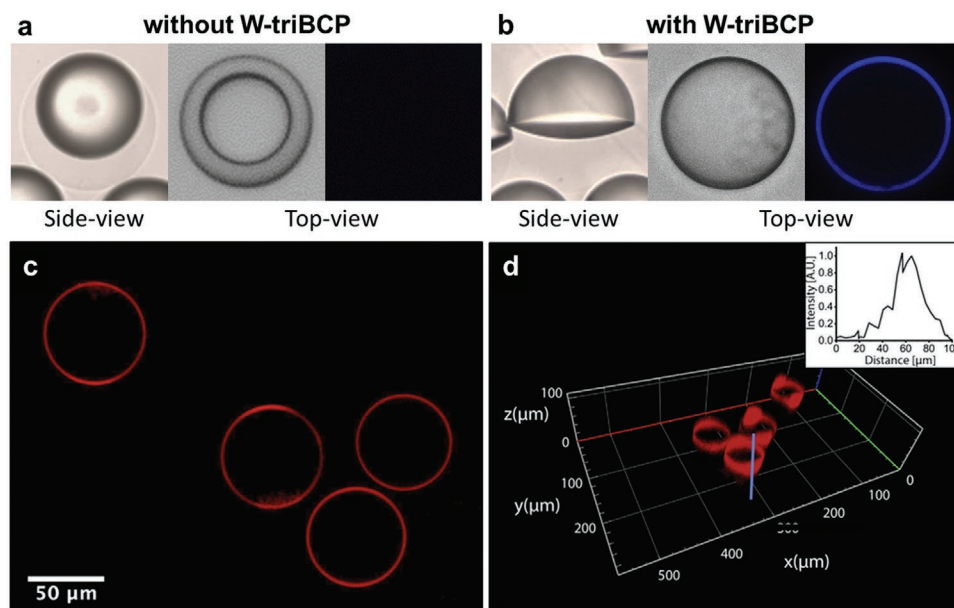


**Figure 4.** Side-view and top-view bright-field and fluorescence microscopy images of biphasic emulsions a) without polymer, and b) containing 0.15 wt% of W-triBCPs. c) 2D and d) 3D fluorescence microscopy images of triBCP localized on the biphasic emulsions. The 3D images were obtained by z-stacking 2D images at different focal depths. Inset shows the line profile measured across the XZ plane.

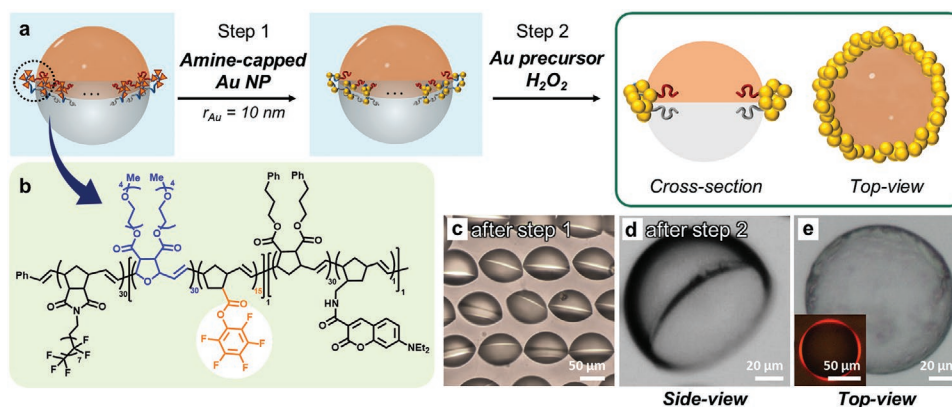


**Figure 5.** a) Schematic illustration of the experimental process to fabricate a gold ring along the triphase junction. b) Chemical structure of polymer having pentafluorophenol esters group (PFP-W-triBCP) to covalently link amine-functionalized PEGylated Au seed NPs. c) Low-magnification, side-view optical microscopy image of Janus emulsions anchored with PFP-W-triBCPs and amine-capped Au seed NPs (after Step 1). d) Side-view and e) top-view transmittance optical microscopy images of gold ring-decorated Janus emulsions (after Step 2). The inset figure is the corresponding reflectance optical microscopy image of (e).

strength of the polymers (Figure S6, Supporting Information). Amine-functionalized Au NPs were covalently linked to the PFP-W-triBCP moiety as illustrated in **Figure 5a,c**. In this process, we first fabricated monodisperse Janus emulsions containing PFP-W-triBCPs (0.2 wt%) using a 100  $\mu\text{m}$  sized microfluidic chip. An aqueous solution of 20 nm sized amine-functionalized PEGylated Au NP ( $50 \mu\text{L mL}^{-1}$ , Figure S7, Supporting Information) was then added to the Janus emulsions (Step 1 in Figure 3a). After 3 d, the electroless Au deposition process was followed to increase the size of the Au NPs (Step 2 in Figure 3a).<sup>[15]</sup> Figure 5d,e shows the transmittance and reflectance optical microscopy images of the resultant gold ring-decorated Janus emulsions.

To elucidate the detailed nanostructure of the gold ring, we prepared a series of emulsions with different concentrations of Au precursor (i.e., 1, 5, and 10  $\text{mg mL}^{-1}$ , Step 2 in Figure 3a) or

different concentrations of amine-functionalized Au NP seeds (i.e., 10, 20, and 50  $\mu\text{L mL}^{-1}$ , Step 1 in Figure 3a), and after removal of all liquids, we characterized the residual particles deposited by scanning electron microscopy (SEM). As the concentration of the Au precursor increased from 1 to 10  $\text{mg mL}^{-1}$ , the radius of individual Au NP ( $r_{\text{Au}}$ ) increased from 10 to 105 nm (**Figure 6c–e**). Although solvent evaporation results in nonuniform particle distribution, we observed that the average thickness of the gold ring was controllable by adjusting the ratio of polymer to Au NPs (**Figure 6f–h**). Interestingly, upon deposition of gold rings, the color was observed under an optical microscope in reflectance mode (**Figure S8**, Supporting Information).

Microscale concave interfaces allow for the formation of structural color by total internal reflection (TIR) and interference of incident white light, an effect which was first

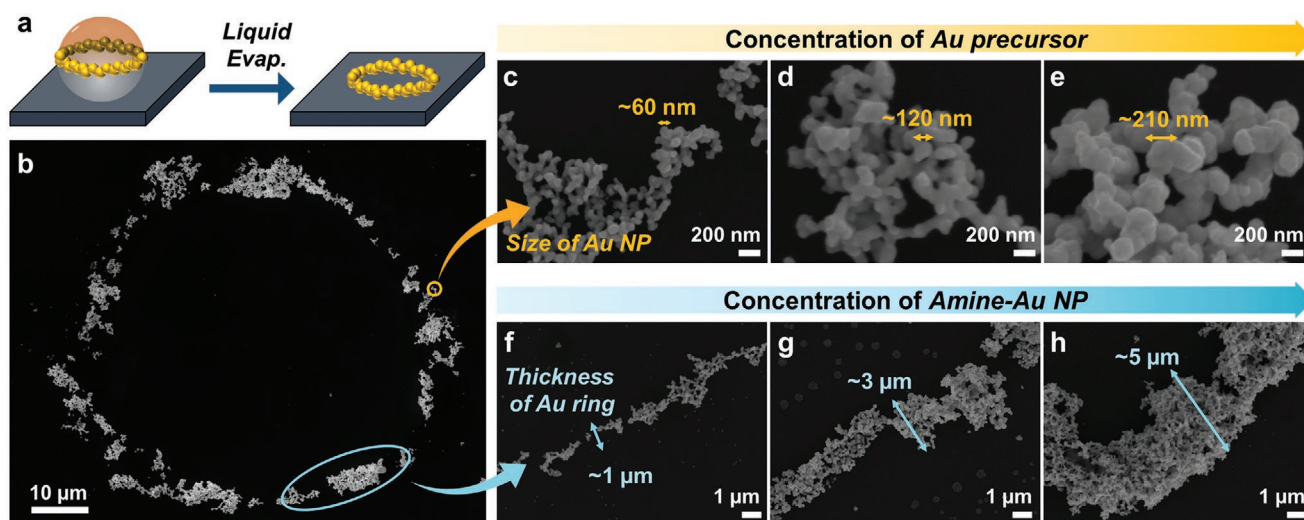


**Figure 6.** a) Schematic illustration to characterize the gold ring. b) SEM image of the gold ring after evaporation of all liquids. c–e) Effect of Au precursor solution on the size of individual Au NP: SEM images of gold ring prepared with different concentrations of Au precursor (1, 5, and 10  $\text{mg mL}^{-1}$ ) at a fixed amount of Au NPs ( $20 \mu\text{L mL}^{-1}$ ). f–h) Effect of amine-functionalized Au NP on the thickness of gold ring: SEM images of gold ring prepared with different concentrations of Au NP (10, 20, and 50  $\mu\text{L mL}^{-1}$ ) at a fixed concentration of Au precursor (5  $\text{mg mL}^{-1}$ ).

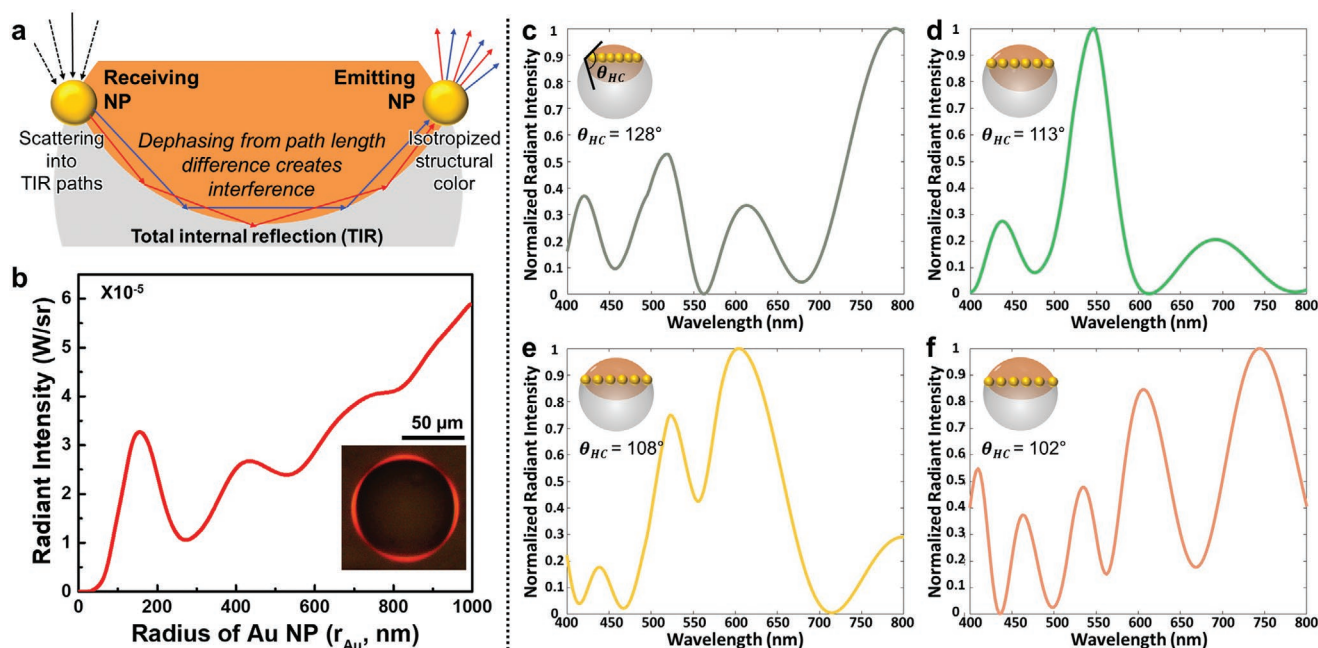


**Figure 7.** a) Schematic illustration showing the effects of Au NP light scattering on total internal reflection (TIR) and isotropization of the emitted interference-filtered light. b) A plot of the reflected radiant intensity from TIR created by light scattered from the entire gold ring as a function of the Au NP radius. Inset is the reflective optical microscope images of Janus emulsion functionalized with PFP-W-triBCP surfactant and 200 nm sized Au NPs. c–f) Theoretically calculated normalized reflecting color spectra of gold ring-decorated Janus emulsions with different contact angles ( $\theta_{HC}$ ) of c) 128°, d) 113°, e) 108°, and f) 102°. For calculation, we used the emulsion diameter of 86  $\mu\text{m}$  and the Au NP radius of 100 nm, where the direction of incidence and observation were taken normal to the gold ring. The color represented by the trace was obtained by converting the intensity spectra into CIE color space.

quantified in biphasic emulsions (see Supporting Information for schematic details of how this structural color arises from interference).<sup>[7a]</sup> This phenomenon is dependent on the curvature of the emulsions' internal interface and the emulsion size. Without the gold being present, the observed colors strongly depend on the angle of incidence and the observation conditions. This iridescent behavior makes renders such a platform impractical as a colorimetric indicator of droplet morphology. We find that the gold ring leads to an enhancement of this structural color effect in two different ways: 1) The Au NPs in the ring at the triphase junction act as antennas receiving the light from a wide range of incidence directions and scattering a substantial fraction onto a set of total internal reflection trajectories along the emulsions' internal interface. 2) The Au NPs facilitate the observation of the interference filtered light, as after traversing the cavity and undergoing interference, the light is scattered again by the Au NPs, which now act as emitting antennas with a considerable angular breath (Figure 7a). This leads to several advantages compared to the case without Au NPs: substantially more light is undergoing TIR and interference, and the effect is much less dependent on the angle of incidence and the observation direction.

To analyze the observed structural color and specify the gold ring's impact on it, we analytically derived an expression for the light scattered back at the triphase interface. A key feature is that Au NPs scatter light strongly with an angular distribution centered about the incoming light ray direction.<sup>[16]</sup> A fraction of these scattered rays transmits into the HC phase and undergo TIR at the HC/FC interface. Rays scattered at different angles

have different path lengths (and hence, phase differences) when exiting the emulsion (Figures S10–S14, Supporting Information). The interference between these rays results in the structural color seen at the emulsion interface. By summing the complex amplitude of all the possible light ray trajectories that contribute to TIR, the intensity of the light exiting the droplet can be analytically calculated as a function of wavelength (see Supporting Information for a detailed treatment of the numerical model used). Using these calculations, we can analyze and predict the intensity of TIR created from the entire gold ring (Figure 7b) and reflecting color depending on the geometry of emulsion (Figure 7c–f).

There are several key points to be highlighted regarding the structural color obtained using this material system. First, the triblock nature of the polymer surfactant is critical for obtaining triphase-localized gold rings and consequently the structural color. It is important to note that a random decoration of particles would not give rise to a strong structural color effect. This can be rationalized since a) the fraction of light collected and scattered back would be much lower as a result of multiple scattering events in random directions and b) the interference that gives rise to structural color would not occur. The path length difference between the scattered rays in the concave cavity will be much longer than the coherence length of the light source (up to 5–10  $\mu\text{m}$ ). Moreover, in stark contrast to intrinsic TIR at the HC/FC interface, the Au NPs scatter light over a broad angular range over a set of TIR trajectories for any given angle incidence, and as a result, the reflected color is significantly less dependent on the angle of observation.<sup>[7a]</sup> This

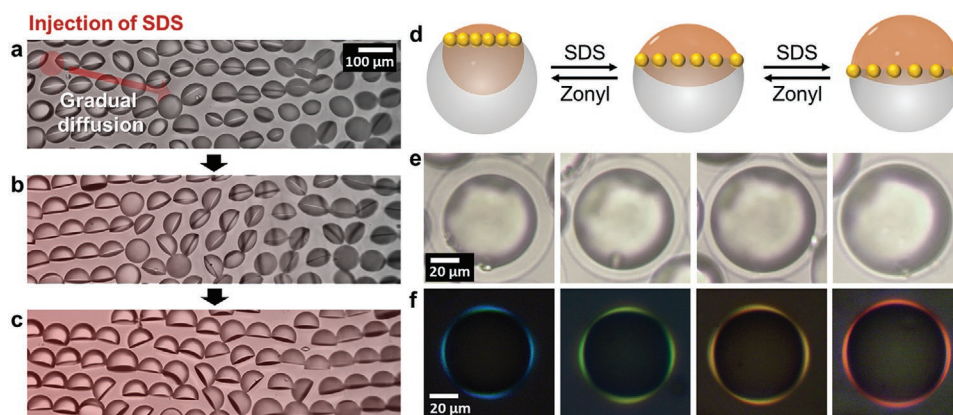


**Figure 8.** a–c) Side-view optical microscopy images of homogenous, gold ring-decorated Janus emulsions captured at intervals of 5 s after injecting concentrated SDS solution (1 wt%). The dark phases are HC, and the transparent phases are FC. d) Illustration of the dynamic reconfiguration of biphasic emulsions with changes in surfactant concentration. e) Top bright-field view with an optical microscope (transmission) of a progression in the emulsion from a nearly core/shell structure to the perfect Janus. f) Reflection colors from the corresponding emulsions shown in (e).

also affords TIR interference even for the emulsion geometries where the coloration would not be observed without the Au NP for a given incidence and observation geometry. Therefore with this functional scheme, the color of the droplets strongly correlates to only the droplet size and morphology, thus providing an opportunity to realize a versatile platform for the angle-free colorimetric sensing.

### 2.3. Dynamic Optical Behavior of Gold Ring-Functionalized Complex Emulsion

Biphasic emulsions have characteristically responsive surfaces that dynamically reconfigure in response to their surrounding chemical environment. The microscale concave interface with enhanced TIR interference by Au NP scattering enables the strong coloration of emulsions. Finally, dynamic reconfiguration of the gold ring-containing biphasic emulsions is readily achieved through changes in HC/FC surfactant mass balance. Low magnification side-view images were captured at intervals of 5 s after injecting concentrated sodium dodecyl sulfate (SDS, anionic HC surfactant). A gradual increase of SDS caused a morphology change to perfect Janus as visualized in Figure 8a–c. A decrease of the contact angles ( $\theta_{HC}$ ) occurs and the reflecting color is red-shifted (i.e., from blue to green, yellow, and red at 128°, 113°, 108°, and 102°, respectively (Figure 8d–f). The structural color is highly sensitive to the contact angle of the interface, as a result of the changes in both relative amplitude and phase contributions of the different ray trajectories participating in TIR. Our experimental observations are consistent with the spectra predicted in Figure 7c–f, providing a proof-of-concept system for a colorimetric optical transducer.

## 3. Conclusion

In this contribution, we presented a concept for localizing functional polymer surfactants at the triphase junction of biphasic emulsions to control the emulsion's morphology and

optical behavior. Specifically, an interfacial assembly of triBCPs created a dense polymer ring along the hydrocarbon/fluorocarbon/water interfacial line. The presence of these polymers at the triphase line also allowed us to assemble a gold ring around the emulsion by localizing Au NPs through covalent binding to the triBCPs modified with reactive esters. These particles readily funnel light into a range TIR trajectories via scattering and isotropize the structural colors produced by interference at the internal, concave interface of the emulsion droplets, which can enable real-time determination of droplet size and shape via the specific reflected color. We provide a theoretical model to explain the influence of the gold ring on the emulsion structural colors, suggesting a tool to rationally quantify emulsion configuration in colorimetric sensing scenarios conceived around stimuli-responsive, reconfigurable emulsions.

## 4. Experimental Section

**Materials:** Diethylbenzene, Zonyl FS-300 (Zonyl, 40% solids), sodium dodecyl sulfate (SDS, 99%), gold(III) chloride hydrate ( $\text{HAuCl}_4$ , >99%), hydrogen peroxide ( $\text{H}_2\text{O}_2$ , 35%), and amine-functionalized PEGylated Au NP ( $M_n = 3000$ , diameter = 20 nm) were purchased from Sigma-Aldrich and used as received. 2-(trifluoromethyl)-3-ethoxydodecafluorohexane (HFE-7500) was purchased from Synquest and used as received. All chemicals used in the preparation of the polymers were obtained from commercial sources (Sigma-Aldrich, Oakwood Chemicals, Tokyo Chemical Industry, Alfa Aesar) and used as received. See the Supporting Information for details.

**General Procedure for the Synthesis of triBCPs (W-, HC-, FC-, and PFP-W-triBCPs):** In argon flushed, septum capped vials, stock solutions of Grubbs' third generation catalyst (G3), and each monomer were prepared in dry, argon-sparged chloroform (anhydrous chloroform was obtained by drying over 4Å molecular sieves). A two-dram vial with a Teflon-coated magnetic stir bar was sealed with a septum and flushed with argon. The vial was then charged with G3 (4.5 mg, 0.0055 mmol) in 1 mL of chloroform. Monomers were added in 1.5 mL aliquots of dry, argon-sparged chloroform. Intervals between additions were 5 min for the first block, 10 min for the second, and 10 min for the final block, before quenching with 50  $\mu\text{L}$  of ethyl vinyl ether. Solutions were concentrated to  $\approx 1$  mL and added dropwise to diethyl ether to precipitate

the polymer and the resulting material collected by centrifugation (7000 RPM, 5 min). The resulting material was redissolved in 1 mL of chloroform added and precipitated into diethyl ether and collected by filtration. The resulting greenish solid was dried to yield the surfactant polymer.

**Generation of Biphasic Emulsion:** A DCM solution (1 wt%) of W- (or HC-, FC-) triBCP was prepared. A calculated amount of polymer solution was added to the mixture of diethylbenzene (2 mL) and HFE-7500 (2 mL), where the final concentration of triBCPs was adjusted in a range of 0.01 to 0.3 wt%. The organic solution containing triBCP was heated to above the suspension's low upper critical solution temperature ( $T_c$ ) to allow the liquids to form a homogeneous mixture and DCM to evaporate. Then, the mixture was emulsified in an aqueous solution containing 0.5 wt% of Zonyl using a microfluidic device purchased from Dolomite Microfluidics. A Telos 2 Reagent Chip (100  $\mu$ m) was used, and the pressures of the continuous phase and dispersed phase were controlled to 1000 and 500 mbar, respectively. To induce the phase separation, we cooled down the droplet temperature for about 30 min.

**Fabrication of Gold Ring Along the Triphase Interface:** PFP-W-triBCP was dissolved in DCM and used for the preparation of Janus emulsions as described in the general procedure for biphasic emulsions. An aqueous solution (1 mL) of amine-functionalized PEGylated Au NPs (diameter = 20 nm, 10 to 50  $\mu$ L) was added to the dispersion of Janus emulsions to initiate covalent attachment. After 3 d, an aqueous solution containing HAuCl<sub>4</sub> (1 to 10 mg mL<sup>-1</sup>) and H<sub>2</sub>O<sub>2</sub> (0.05 wt%, 3 to 4 drops) was added to the Au NP-decorated Janus emulsions to realize the electroless deposition process, and the reaction was kept going for 20 min. Dissociated Au NPs and all reagents were removed by repeated washing steps.

## Supporting Information

Supporting Information is available from the Wiley Online Library or from the author.

## Acknowledgements

K.H.K. and B.R.M. contributed equally to this work. The authors are grateful for support from a Vannevar Bush Faculty Fellowship (Grant No. N000141812878) from the Department of Defense. B.R.M. thanks the MIT MLK Visiting Professors and Scholars Program for support.

## Conflict of Interest

The authors declare no conflict of interest.

## Data Availability Statement

Research data are not shared.

## Keywords

complex emulsions, gold rings, structural colors, triblock copolymer surfactants, triphase interface

Received: November 27, 2020

Revised: January 6, 2021

Published online: February 19, 2021

- [1] a) Y. Lin, H. Skaff, T. Emrick, A. D. Dinsmore, T. P. Russell, *Science* **2003**, 299, 226; b) J. Forth, P. Y. Kim, G. Xie, X. Liu, B. A. Helms, T. P. Russell, *Adv. Mater.* **2019**, 31, 1806370; c) K. Piradashvili, E. M. Alexandrino, F. R. Wurm, K. Landfester, *Chem. Rev.* **2016**, 116, 2141.
- [2] Y. Y. Song, J. B. Fan, S. T. Wang, *Mater. Chem. Front.* **2017**, 1, 1028.
- [3] a) M. J. Felipe, N. Estillore, R. B. Pernites, T. Nguyen, R. Ponnappati, R. C. Advincula, *Langmuir* **2011**, 27, 9327; b) D. K. Beaman, E. J. Robertson, G. L. Richmond, *Langmuir* **2011**, 27, 2104; c) E. J. Robertson, G. L. Richmond, *Langmuir* **2013**, 29, 10980.
- [4] a) L. Hu, M. Chen, X. Fang, L. Wu, *Chem. Soc. Rev.* **2012**, 41, 1350; b) P.-P. Fang, S. Chen, H. Deng, M. D. Scanlon, F. Gumy, H. J. Lee, D. Momotenko, V. Amstutz, F. Cortés-Salazar, C. M. Pereira, Z. Yang, H. H. Girault, *ACS Nano* **2013**, 7, 9241.
- [5] a) M. D. Scanlon, E. Smirnov, T. J. Stockmann, P. Peljo, *Chem. Rev.* **2018**, 118, 3722; b) Y. Montelongo, D. Sikdar, Y. Ma, A. J. S. McIntosh, L. Velleman, A. R. Kucernak, J. B. Edell, A. A. Kornyshev, *Nat. Mater.* **2017**, 16, 1127; c) E. Smirnov, P. Peljo, M. D. Scanlon, H. H. Girault, *ACS Nano* **2015**, 9, 6565; d) M. K. Bera, H. Chan, D. F. Moyano, H. Yu, S. Tatur, D. Amoanu, W. Bu, V. M. Rotello, M. M. Meron, P. Král, B. Lin, M. L. Schlossman, *Nano Lett.* **2014**, 14, 6816.
- [6] a) L. D. Zarzar, V. Sresht, E. M. Sletten, J. A. Kalow, D. Blankschtein, T. M. Swager, *Nature* **2015**, 518, 520; b) C. A. Zentner, F. Anson, S. Thayumanavan, T. M. Swager, *J. Am. Chem. Soc.* **2019**, 141, 18048; c) L.-Y. Chu, A. S. Utada, R. K. Shah, J.-W. Kim, D. A. Weitz, *Angew. Chem., Int. Ed.* **2007**, 46, 8970; d) Y. He, S. Savagatrup, L. D. Zarzar, T. M. Swager, *ACS Appl. Mater. Interfaces* **2017**, 9, 7804; e) L. Ge, S. E. Friberg, R. Guo, *Curr. Opin. Colloid Interface Sci.* **2016**, 25, 58; f) L. R. Shang, Y. Cheng, Y. J. Zhao, *Chem. Rev.* **2017**, 117, 7964; g) A. Perro, C. Nicolet, J. Angy, S. Lecommandoux, J. F. Le Meins, A. Colin, *Langmuir* **2011**, 27, 9034.
- [7] a) A. E. Goodling, S. Nagelberg, B. Kaehr, C. H. Meredith, S. I. Cheon, A. P. Saunders, M. Kolle, L. D. Zarzar, *Nature* **2019**, 566, 523; b) S. Nagelberg, L. D. Zarzar, N. Nicolas, K. Subramanian, J. A. Kalow, V. Sresht, D. Blankschtein, G. Barbastathis, M. Kreyling, T. M. Swager, M. Kolle, *Nat. Commun.* **2017**, 8, 14673; c) X. Wang, Y. Zhou, Y.-K. Kim, M. Tsuei, Y. Yang, J. J. de Pablo, N. L. Abbott, *Soft Matter* **2019**, 15, 2580; d) C.-J. Lin, L. Zeininger, S. Savagatrup, T. M. Swager, *J. Am. Chem. Soc.* **2019**, 141, 3802; e) L. Ge, W. Tong, Q. Bian, D. Wei, R. Guo, *J. Colloid Interface Sci.* **2019**, 554, 210.
- [8] a) L. D. Zarzar, J. A. Kalow, X. P. He, J. J. Walish, T. M. Swager, *Proc. Natl. Acad. Sci. USA* **2017**, 114, 3821; b) L. Zeininger, S. Nagelberg, K. S. Harvey, S. Savagatrup, M. B. Herbert, K. Yoshinaga, J. A. Capobianco, M. Kolle, T. M. Swager, *ACS Cent. Sci.* **2019**, 5, 789; c) Q. F. Zhang, S. Savagatrup, P. Kaplonek, P. H. Seeberger, T. M. Swager, *ACS Cent. Sci.* **2017**, 3, 309.
- [9] A. Concellón, C. A. Zentner, T. M. Swager, *J. Am. Chem. Soc.* **2019**, 141, 18246.
- [10] a) P. Raffa, D. A. Z. Wever, F. Picchioni, A. A. Broekhuis, *Chem. Rev.* **2015**, 115, 8504; b) T. Taddese, P. Carbone, D. L. Cheung, *Soft Matter* **2015**, 11, 81; c) J. J. Armao, I. Nyrkova, G. Fuks, A. Osypenko, M. Maaloum, E. Moulin, R. Arenal, O. Gavati, A. Semenov, N. Giuseppone, *J. Am. Chem. Soc.* **2017**, 139, 2345; d) N. Saleh, T. Phenrat, K. Sirk, B. Dufour, J. Ok, T. Sarbu, K. Matyjaszewski, R. D. Tilton, G. V. Lowry, *Nano Lett.* **2005**, 5, 2489; e) J. C. Baret, F. Kleinschmidt, A. El Harrak, A. D. Griffiths, *Langmuir* **2009**, 25, 6088.
- [11] R. B. Grubbs, R. H. Grubbs, *Macromolecules* **2017**, 50, 6979.
- [12] a) C. Slugovc, *Macromol. Rapid Commun.* **2004**, 25, 1283; b) A. Leitgeb, J. Wappel, C. Slugovc, *Polymer* **2010**, 51, 2927; c) C. W. Bielawski, R. H. Grubbs, *Prog. Polym. Sci.* **2007**, 32, 1.
- [13] a) Y. M. Liu, X. Zhang, *Chem. Soc. Rev.* **2011**, 40, 2494; b) Y. Zhai, Y. Ma, S. N. David, D. Zhao, R. Lou, G. Tan, R. Yang, X. Yin, *Science*



- 2017, 355, 1062; c) J. B. Edel, A. A. Kornyshev, A. R. Kucernak, M. Urbakh, *Chem. Soc. Rev.* **2016**, 45, 1581.
- [14] a) E. Blasco, M. B. Sims, A. S. Goldmann, B. S. Sumerlin, C. Barner-Kowollik, *Macromolecules* **2017**, 50, 5215; b) D. D. Manning, L. E. Strong, X. Hu, P. J. Beck, L. L. Kiessling, *Tetrahedron* **1997**, 53, 11937; c) M. D. McKenna, J. Barberá, M. Marcos, J. L. Serrano, *J. Am. Chem. Soc.* **2005**, 127, 619.
- [15] a) A. L. Tasker, S. Puttick, J. Hitchcock, O. J. Cayre, I. Blakey, A. K. Whittaker, S. Biggs, *J. Mater. Chem. B* **2018**, 6, 2151; b) K. H. Ku, J. Li, K. Yoshinaga, T. M. Swager, *Adv. Mater.* **2019**, 31, 1905569.
- [16] a) G. Mie, *Ann. Phys.* **1908**, 330, 377; b) C. F. Bohren, D. R. Huffman, *Absorption and Scattering of Light by Small Particles: Absorption and Scattering by an Arbitrary Particle*, Wiley, New York **1983**.